JOURNAL OF CATALYSIS 153, 275–292 (1995)

The Nature of the Active Phase in the Heteropolyacid Catalyst $H_4PVMo_{11}O_{40} \cdot 32H_2O$ Used for the Selective Oxidation of Isobutyric Acid

Th. Ilkenhans, B. Herzog, Th. Braun, and R. Schlögl[1]

Fritz Haber Institut der Max-Planck Gesellschaft, Faradayweg 4-6, D-14195 Berlin, Germany

Received February 2, 1994; revised January 17, 1995

The structural changes of the title compound during heating and under conditions of catalytic conversion of isobutyric acid to methacrylic acid were followed *in situ* by powder X-ray diffraction under continuous control of its activity. The results were verified by a postmortem phase analysis of practical supported catalyst samples used in kinetic reactors. The activity of the catalyst is correlated with its dehydrated form. A new cubic phase of a water-free vanadyl salt of the heteropolyacid (HPA) was found to be connected to a maximum conversion. This phase is isostructural to the unsubstituted anhydrous alkali-3-HPA salts and is metastable at ambient conditions with respect to rehydration. The catalyst material as a whole is metastable at any temperature above the onset of conversion with respect to a partially reversible decomposition into MoO_3 and amorphous other components. Restructuring into crystalline forms of HPA is possible from the deactivated material upon dissolution and recrystallization at 323 K. *In situ* UV–VIS data and X-ray diffraction show the complete self-reorganization of the MoO_3 phase and the amorphous V and P compounds into new Keggin anions indicating the possible living nature of the catalyst under reaction conditions which enable extended lifetimes beyond the stability limits found in the present *in situ* X-ray diffraction experiments.

INTRODUCTION

The title compound (A1 in Fig. 3 and Table 1) is a member of the family of heteropolyacid (HPA) catalysts (1) with fully hydrated Keggin anions (2) in its room temperature form. Its combination of strong Brønsted acidity with high redox activity renders this HPA a good catalyst for the selective oxidehydrogenation of isobutyric acid (IBA) to methylacrylic acid (MAA) (3) which has now reached the stage of pilot plant testing for commercial application. Significant problems with long-term deactivation and insufficient selectivity (4) were not solved up to now despite many efforts to promote the HPA with, e.g., copper and alkali. In the early development it was noted (3) that the presence of vanadium in a limited range of compositions enhances the activity and selectivity of the HPA but leads to a reduced structural stability.

In a recent paper (5) the room temperature single crystal structures of several HPA samples were determined. The samples were prepared from binary oxide mixtures via the technical hydrothermal synthesis route. The HPA catalysts may be either of the Keggin structure or of the inverse Keggin structure, a disorder modification with severe consequences for the packing of the anions within the crystal. In both structures the primary Keggin anions are of similar constitution, exposing two different species of oxygen anions in terminal and bridging configurations at the molecular surface. The substitutional element vanadium could not be localized and did not lead to any discernible distortion of the anionic structure.

The structural parameters of these HPA catalysts are largely determined by the hydration water network between the anions and not by the Keggin anion structure. The thermal stability of the water network (6) depends on the surface charges and hence on the substitution and nature of the counterions. As water is also present as a reaction product and as an additive in the reaction mixture, the participation of this water shell of the Keggin anions in the catalytic action is a plausible hypothesis. The participation of well-defined solvation structures (7) or of a "pseudoliquid" phase (8) was discussed in the literature. These models place HPA catalysts in the class of microporous materials in which the hydration water indicates the access of polar substrate molecules to the total molecular surface of the Keggin anions.

With this background the crystal structure and the degree of hydration of the active HPA catalyst under reaction conditions are of significant interest. The behavior of the materials under thermal load *in situ* and after con-

[1] To whom correspondence should be addressed.

0021-9517/95 $6.00

tact with IBA/oxygen was studied recently by X-ray diffraction (9) and vanadium NMR (10). It was found that two regions of water loss terminating at 450 and 600 K exist with the latter dehydration of "constitutional" (11) water leading to an expulsion of the vanadium into the secondary structure in a highly symmetrically coordinated form located in the counterion shell of the anion. It was also stressed that an intermediate amorphous form (9) identified by its morphology (12) above the second water evolution and before structural disintegration into MoO_3 was related to the catalytic action of the HPA in the IBA oxydehydration. In other publications (1, 13) the existence of hydrated forms of Keggin anions in the catalytically active form was taken for granted. The mode of action of the vanadium promoter is ascribed to a modification of the electronic structure influencing the redox potential of the HPA relative to the organic substrate; vanadium is seen (13) as an electronic promoter.

Powder X-ray diffraction is a bulk-sensitive technique with no obvious relevance to surface catalytic processes. In order to verify a connection between structural results and catalytic behavior the present *in situ* experiments were conducted with continuous monitoring of the activity and selectivity of the catalyst during its exposure to the IBA/water/oxygen mixture. Comparison of the structural findings with those of a reference experiment using the vanadium-free parent HPA $H_3PMo_{12}O_{40}$, which is known to be a less active IBA oxidehydrogenation catalyst than the system A1, was used to verify the assignment of the active phase.

Establishing the correlation between bulk structure and reactivity is of particular significance for the present systems as it was shown very clearly (14) that partly neutralized HPA used for acrolein oxidation may decompose into fully neutralized supports, molybdenum oxides, and a surface film of free acid which would be undetectable by XRD. These considerations led us also to study unsupported catalysts as in previous conversion studies (4) although in other experiments (13) and in technical practice, supported catalysts were used.

EXPERIMENTAL

The catalyst material (phase A1) was prepared from binary oxides using the hydrothermal synthesis method. Appropriate amounts of binary oxides were dissolved at 363 K at pH 1.2 and the resulting 0.1 N solution of the desired HPA was then precipitated by distilling off water. All steps were controlled by *in situ* UV–VIS spectroscopy allowing the optimization of reaction parameters in such a way as to obtain a minimum of undesired by-products, which were, according to ^{31}P NMR data for the $PVMo_{11}$ material, less than a few percent. Powder diffraction, FTIR, solid state ^{51}V NMR, TG, and SEM/EDX were used to verify the composition and structure of the room temperature precursor. Its high resolution powder diffraction pattern is given in Ref. (5). *Ex situ* XRD data were taken with STOE STADI P diffractometer in focusing transmission geometry using monochromatic Cu$K\alpha$ radiation and a position-sensitive detector. Samples were held in glass capillaries sealed in air rapidly after the respective treatment.

The *in situ* XRD setup is described in detail elsewhere (15). Briefly, we use a modified Bühler camera with special gas inlets and a modified cooling system housing a stainless-steel sample holder (no background reaction). Diffraction properties (position, linewidth, intensity loss due to thermal drift) are calibrated against Si as internal standard. A STOE STADI P Bragg–Brentano diffractometer with a scintillation counter and Cu$K\alpha$ radiation was used in the present experiments. The lattice parameters were obtained from fits of the corrected and background-subtracted raw data profiles.

Reaction monitoring was done using a Balzers QMG 400 mass spectrometer interfaced with a heated capillary to the outlet of the camera. The relevant gas components, IBA, MAA, and the main side product acetone (ACE), were discernible by their fragmentation patterns. Mass 86 was used after corrections for cross-contributions to follow the conversion to MAA. The feed mixture was IBA : water 1 : 9, LHSV 1.01 or 2.5 liters/min applied via a pulsation-free pump and an evaporation system excluding the delivery of liquids into the chamber cofed with a stream of nitrogen/oxygen 40 : 80 ml/h. The absolute conversions at 573 K were 0.33 mmol/h at LHSV 1.01 and 0.44 mmol/h at 2.5 LHSV inside the *in situ* X-ray camera. No conversion was observed with the prepassivated camera/sample holder assembly.

Experiments were done with preconditioned samples constantly kept in 80 mbar moisture inside the chamber to reach the full hydration stage of the phase (A1). Heating was done either in air (thermal load) or in the reaction feed gas (conversion runs). Preexperiments with non-steady-state conditions were used to determine the temperatures of the changing structures. The main experiments were done with a strictly reproducible time–temperature profile including holding periods of 2 h at any temperature (interval 10 to 30K) for allowing the system to reach a stable performance. This was not possible at temperatures above 640 K. Thermal load experiments were further conducted *ex situ* with the specimen heated in dry oxygen to the desired temperatures for 24 h and then sealed during cooling to prevent rehydration which is a rapid process occurring for dehydrated bulk samples within minutes in ambient air. These experiments led to the same structural parameters as the *in situ* experiments but the diffraction patterns of the single phase products were of superior quality compared to those in the *in situ* experiments which

cannot unambiguously be assigned to a different crystal quality as the conditions of data collection were different.

SEM/EDX analysis was done on a JEOL JSM 35 instrument with an HNU system 5000 analyzer with gold-coated samples at 25 keV under a vacuum of better than 1×10^{-6} mbar. EDX spectra were collected for 100 s each and treated by the standard ZAF analysis.

IMR–MS analyses were done with a microreactor setup, coupled to an IMR–MS 100 instrument from Atomika operating with Kr as the primary ion source. Purified nitrogen was used as a carrier gas. The catalyst powders were dehydrated together with the reactor system to remove water and oxygen from the loading procedure. The catalysts were converted to phase B during this procedure, as was substantiated by XRD analysis.

TGA analyses were conducted with a Perkin–Elmer TGS 2 system using a quartz crucible and using dried helium at 100 ml/min as the carrier gas. This gas stream converted the samples at 300 K into phase A2 and the temperature ramp was started only after reaching constant weight at room temperature.

RESULTS

Conversion Experiments

The present system may be considered as a microdifferential reactor with different catalytic properties from the fixed bed systems used in the kinetic work in the literature. No direct comparison between the two sets of experiments is thus possible.

In Fig. 1 characteristic mass spectra are compiled for a conversion experiment (trace A, 553 K, maximum water partial pressure) and pure reference materials. Quantitative analysis reveals that under these conditions about 50% conversion with 50% selectivity to MAA was reached. The main by-products were acetone with 42% selectivity and a small abundance of propene. Typical results in an integral reactor with our catalyst under our conditions (4) were 75% conversion with selectivities to MAA of 68.8%, acetone 15.9%, and propene 13.9%. The acetone selectivity was used as a criterion for good operation of our catalyst system, as the wrong conditions, low water partial pressure, or structurally ill-defined catalysts samples led to larger values of the acetone selectivity prior to a reduction in overall conversion.

Conversion-temperature profiles as presented in Fig. 2 for a catalyst load of 2.50 LHSV are useful, however, to document the relative catalytic status of the sample under structural analysis. The profile is structured in five regions of different activity in MAA synthesis. No activity is observed at low temperatures. At 400 K a steep rise leads to a region of relatively stable conversion up to 550 K followed by a second plateau of stable activity at a slightly higher level. At a lower catalyst load the transition into region D is much more pronounced, yielding a 15% increase in conversion. Above 680 K a burst of activity

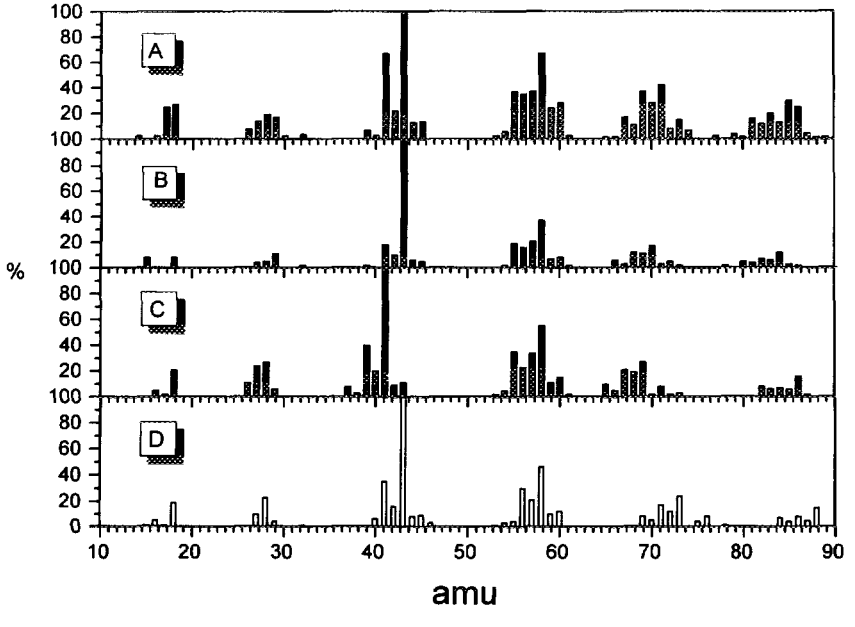

FIG. 1. Schematic representation of characteristic mass spectra obtained from a conversion experiment (trace A) and the relevant reference compounds acetone (trace B), MAA (trace C), and IBA (trace D). The intensity at *m/e* 86 was used to identify the desired product MAA. Conditions: 1×10^{-6} mbar total pressure, 70 eV ionization energy, maximum resolution at *m/e* 70, transfer and mass spectrometer heated to 400 K. The cross sections for *m/e* 86 (product) and *m/e* 88 (educt) were found to be identical within 5% error.

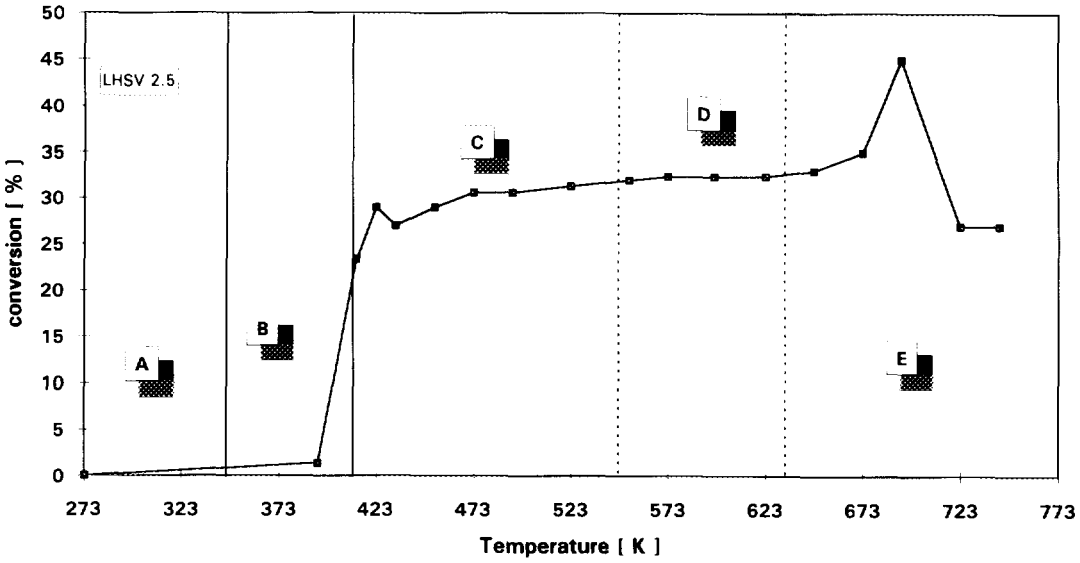

FIG. 2. Conversion vs temperature profile for a catalytic run with ca. 40-mg sample within the *in situ* X-ray diffraction cell. The characters denote the different crystal structures of the catalyst (see also Table 1 and Fig. 3). The empty cell with sample holder was prepassivated for about 48 h at 660 K with the organic feed. After this highly corrosive treatment the conversion of the cell fell to zero. Each data point was reproduced in two independent runs and the conversion was averaged over 2 h under isothermal operation.

leads to a state of rapid deactivation at 700 K. The catalyst operates in practical applications at temperatures around the onset to the second plateau between regions C and D. This temperature is an empirically optimized compromise between optimum-conversion and long enough stability. The activation energy determined in the region of lower stable conversion, 60 kJ/mol, was compatible with literature data (16) from microreactor studies, which indicate for partly cesium-neutralized catalysts, a beginning of catalytic action at 440 K and a maximum steady state conversion at 530 K, in good agreement with the present data. Above 500 K the activation energy for the high LHSV experiments dropped to a value of 22kJ/mol, indicative of a transport limitation which could be traced back to the gas feed geometry of our camera. The geometry could not be optimized because of the transmission of the X-ray beam. It is noted that the system is sensitive to the chemical nature of the catalyst as unsubstituted PMo_{12} led to about 15% less conversion and to 36% MAA selectivity.

These data confirm that we are studying in principle the same catalytic phenomena that occur in fixed bed reactors. They indicate the *in situ* character of the present experiments. This is further substantiated by the time scale of deactivation. In integral reactor experiments (16) the occurrence of a hot spot was described migrating at 553 K with a speed of ca 0.1 cm/h through the catalyst bed. At temperatures between 470 and 640 K we observed stable conversions for several hours and a total deactivation at 553 K within 30 h. At 640 K the catalyst was fully deactivated after 4 h on stream. No stable operation within a time resolution of 1 min was observed above 640 K. The deactivation phenomena were reflected in structural changes detectable by XRD as indicated below.

The not unexpected quantitative disagreement between the catalytic performance of our system and literature data from dedicated kinetic reactors prompted us to test our results in a postmortem analysis of a spent catalyst from a kinetic reactor experiment.

Attempts to run the reaction without cofeeding water were unsuccessful, which we traced back to overloading the catalyst mass (ca. 40 mg) in the reactor in the absence of massive dilution. The XRD patterns indicated the presence of the HPA as a mixture of poorly hydrated Keggin structures with a very large fraction of amorphous material. Postmortem FTIR data showed the absence of the distinct fingerprint lines (17) of well-crystallized Keggin ions below 1050 cm^{-1}. These findings also indicate that active catalysts are well-crystallized and that the occurrence of distinct crystal structures in the XRD may be correlated with the catalytic performance. The active catalyst seems not to be present in an amorphous state, which in fact indicates its deactivation. Structural amorphization detected by Fournier *et al.* (9) and the loss of molybdenum out of the catalyst bed as stated by Haeberle and Emig (16) are compatible descriptions of irreversible deactivation.

The characteristic temperatures of the structural transformations of the HPA were found to be dependent on the gas phase composition. Compared to thermal treatment only, which gave upper limits of these temperatures, the temperature regimes of dehydrated phases changed with

TABLE 1

Structural Parameters of Catalyst Phases (Cell Parameters in pm)

	A1	A2	B	C	D	E
Hydration	32	14	6	2	0	MoO_3
Symmetry	*P4/mnc*	*P*-1	Cubic	Tetragonal[a]	*Pn3m*	*Pb n m*
a	1289	1410	1216	1375.9	1160	369.2
α	90	112.1	90	90	90	90
b	—	1413	—	—	—	1385.5
β	—	109.8	—	—	—	—
c	1844	1355	—	1590.6	—	369.7
γ	90	60.7	—	90	—	90
Initial *T*(K)	300	300	345	420	520	570

[a] Data taken from the literature. Better indexing is possible with lower symmetry; see text and Table 2.

an increased abundance of organic components in the atmosphere and collapsed in a single peak of instability at 460 K and at a LHSV slightly above 2.5.

Crystal Structures

A total of six different crystal structures were detected upon observing the HPA catalysts under reaction conditions. Their temperature regions at which they exist are indicated in Fig. 2. Characteristic parameters and the designations are listed in Table 1. The basic composition for the five HPA structures is $H_4PVMo_{11}O_{40} \cdot n\ H_2O$. The initial temperature given in Table 1 is the temperature at which the respective phase first occurred under thermal treatment. The assignment and structural parameters of the HPA phases A2, B, and C are fully in line with the data given by the paper of Fournier *et al.* (9) and the references therein.

Figure 3 shows the diffraction patterns which were observed for the different phases during a stepwise heating experiment (10 K, 2 h waiting time per step) with simultaneous recording of the conversion of IBA to MAA. The transitions between the highly hydrated phases A1, A2, and B are sharp phase transitions with no total loss of diffracted intensity. The transition between A1 and A2 occurs isothermally by lowering the water partial pressure at 300 K from 100 to 15 mbar. The hexahydrate B is a less well-crystallized phase than the precursors under thermal load and under reaction atmospheres; it could not be obtained in a well-ordered state even when extremely low temperature gradients of 3 K/h were applied. All these hydrated phases are catalytically fully inactive.

The catalytic activity is strongly correlated with the occurrence of the tetragonal phase C, which is the anhydride of the HPA. This phase was indexed in the literature using a tetragonal symmetry with parameters a = 1375.9 pm and c = 1590.6 pm. Close inspection of the diffraction pattern reveals that eight reflections (maximum I/I_0 35%) remain unindexed with the literature parameters (9). The pattern can, however, be fully indexed if the lower symmetry of an orthorhombic system is assumed. Even better agreement between line positions and calculated *d*-values is obtained with hexagonal indexing. In the absence of a full structural analysis we cannot decide on the correct indexing and report all possibilities in Table 2. The lattice parameters for the tetragonal system are used in Table 1.

The term "anhydride" used in the HPA literature is chemically incorrect as the compound still holds water in the form of "constitutional" water. The designation refers to the absence of any crystal water in phase C. For reasons of consistency with the literature we will further use the term anhydride in the following text.

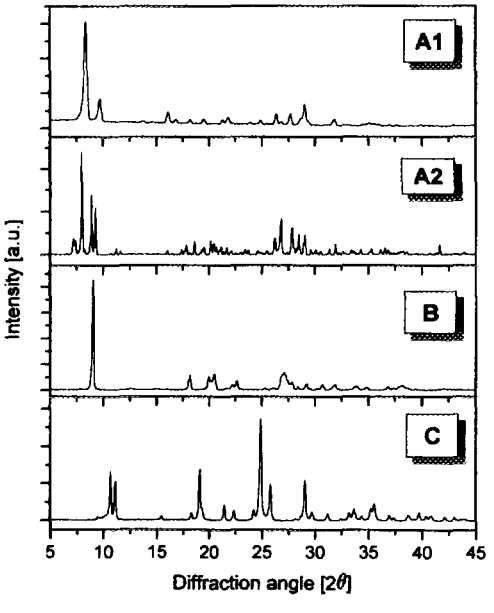

FIG. 3. Powder diffraction patterns of the first four phases occurring during a temperature increase with a step program of 10 K followed by 2 h of isothermal observation. The phase designation is identical to Fig. 2 and Table 1.

TABLE 2

Observed Powder Pattern for Phase C

		T	O	H
2θ	d-value	h k l	h k l	h k l
10.668	8.2861	2 0 1	1 0 1	1 0 2
11.114	7.9547	0 0 2	0 2 0	1 1 0
15.437	5.7353	3 1 1	2 0 1	2 0 2
18.283	4.8485	4 0 0	1 0 2	1 0 4
19.065	4.6513	2 0 3	2 2 1	2 1 2
19.332	4.5876	3 3 0	3 0 0	3 0 0
21.452	4.1389	4 0 2	2 0 2	2 0 4
22.353	3.974	0 0 4	3 2 0	2 2 0
24.23	3.6702	2 0 4	2 2 2	2 1 4
24.838	3.5817	4 0 3	1 3 2	3 1 2
25.784	3.4525	2 2 4	0 0 3	0 0 6
28.634	3.115	6 1 1	1 5 0	3 2 1
29.032	3.0731	4 0 4	1 4 2	3 1 4
29.721	3.0035	3 3 4	3 4 0	4 1 0
31.187	2.8655	6 2 2	4 0 2	4 0 4
32.406	2.7605	6 0 3	3 0 3	3 0 6
33.191	2.6969	7 1 1	4 2 2	3 2 4
33.65	2.6612	4 0 5	5 0 1	5 0 2
34.373	2.6069	1 1 6	3 2 3	2 2 6
35.24	2.5447	7 3 0	1 0 4	1 0 8
35.547	2.5234	7 2 2	5 2 1	4 2 2
36.933	2.4318	6 2 4	5 0 2	4 1 5
37.396	2.4028	8 1 0	5 1 2	5 1 2
38.703	2.3246	8 2 1	5 2 2	4 2 4
39.737	2.2665	6 0 5	3 4 3	4 1 6
40.369	2.2324	7 5 1	3 1 4	3 3 5
40.91	2.2041	8 0 3	6 2 0	5 2 0
42.136	2.1428	9 1 0	1 4 4	3 1 8
42.978	2.1027	9 2 0	4 6 0	3 3 6
43.665	2.0712	8 0 4	0 0 5	0 0 10
44.199	2.0474	4 1 7	1 0 5	1 0 10
45.665	1.985	9 1 3	1 2 5	4 3 5

Note. The indexing is given for a tetragonal (T), orthorhombic (O), or hexagonal (H) system. For a discussion see text. The cell parameters are: (T) a = 19.394 pm, c = 15.992 pm; (O) a = 13.763 pm, b = 15.909 pm, c = 10.377 pm; (H) a = 15.893 pm, c = 20.719 pm.

If the temperature program is continued a new cubic phase, designated D, occurs at 550 K. It is not possible to obtain this structure as single phase under *in situ* conditions, as it is always mixed with the anhydride C. It is pointed out, however, that the second increase in conversion to MAA in Fig. 2 is strictly correlated with the occurrence of sharp reflections of phase D in the diffraction pattern.

An increase in the holding time at temperatures below 570 K also leads to the conversion of the material into phase D. Isothermal *in situ* and *ex situ* preparations revealed that phase D can also be obtained by thermal treatment without catalytic action. The temperature window of its existence is, however, under these conditions limited to 30 K above 660 K. The conditions of catalytic conversion lower the temperature required for its formation by 100 K and widen the range of its existence, which depends on the catalyst load. A diffraction pattern of the new phase prepared *ex situ* is presented in Fig. 4. Phase D can be indexed in the cubic system with reflections listed in Table 3. Additional lines marked in Fig. 4 belong to some anhydride and to sharp reflections of MoO_3 (phase E) in Table 1 and Fig. 2). The *ex situ* diffraction pattern indicates good crystallinity and the phase composition does not change with increased tempering times.

The diffraction pattern of the maximum abundant phase D in the *in situ* experiment is displayed in Fig. 5. It differs from the pattern in Fig. 4 by an overall poorer crystallinity, an increased abundance of the anhydride, the lack of sharp reflections of phase E, and a broad amorphous background indicative of the presence of E as a noncrystalline phase.

The unsubstituted HPA was used in a parallel *in situ* experiment. The same behavior as displayed in Fig. 2 was observed, showing a sharp onset of the catalytic activity with the appearance of the anhydride phase. It formed as a highly crystalline product with the same structural parameters as found for phase C, although no vanadium was present. The diffraction pattern of this vanadium-free anhydride phase F is displayed in Fig. 6. With increasing time on stream the crystallinity became poorer and transformation in the MoO_3 phase E occurred at 590 K within 10 h without going through the stage of phase D. Several

TABLE 3

h k l	2θ	d-values
1 1 0	10.777	8.202
1 1 1	13.209	6.697
2 0 0	15.264	5.8
2 1 1	18.722	4.736
2 2 0	21.651	4.101
3 0 0	22.982	3.867
3 1 0	24.243	3.668
2 2 2	26.597	3.349
3 2 1	28.773	3.1
4 0 0	30.807	2.9
3 3 0	32.726	2.734
3 3 1	33.65	2.661
4 2 0	34.551	2.594
4 2 1	35.432	2.531
3 3 2	36.294	2.473
4 2 2	37.969	2.368
5 1 0	39.582	2.275
5 1 1	40.369	2.232
4 3 2	41.905	2.154
5 2 1	42.656	2.118
4 4 0	44.127	2.051

A = 11.6[Å]
V = 1560.9

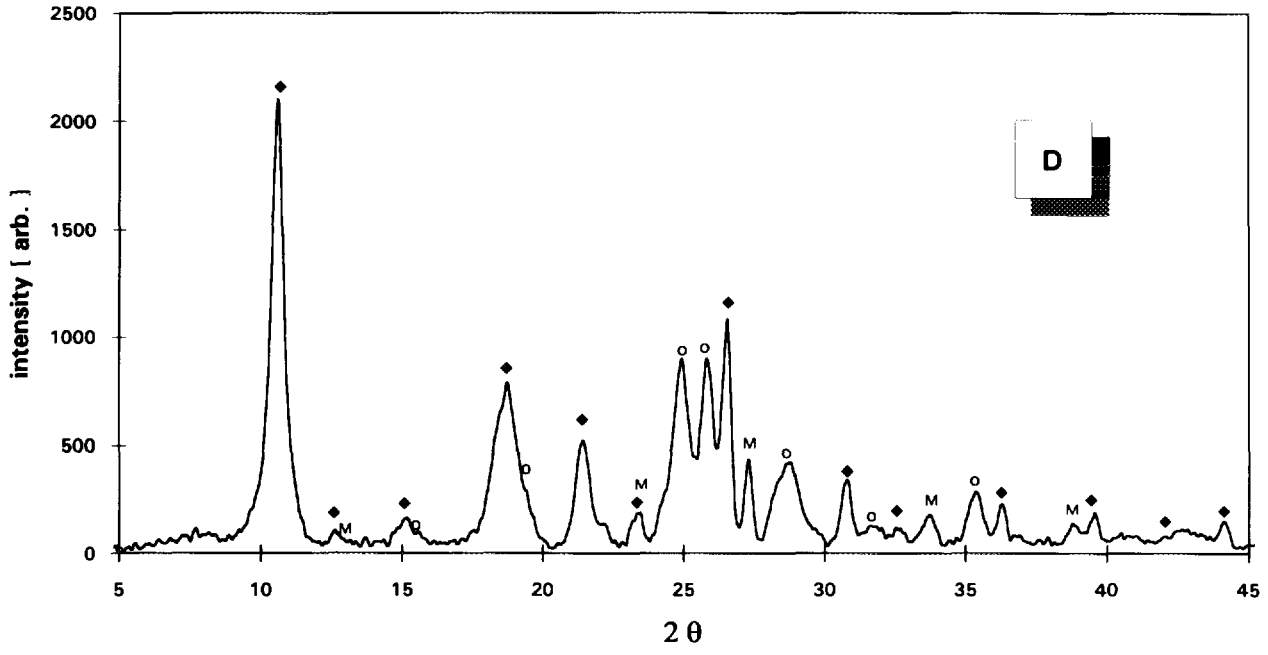

FIG. 4. Powder diffraction pattern of the novel vanadyl-salt phase D prepared *ex situ* by annealing at 600 K in air. The diamonds denote the reflections of the new phase, the open circles indicate the reflections of phase C (the anhydride), and M denotes reflections of phase E (orthorhombic MoO_3).

runs with different heating programs did not reveal the formation of phase D in the vanadium-free system whereas it always occurred with the vanadium-containing HPA. This allows one to conclude that phase D is a vanadyl salt of the HPA. It is isomorphous to alkali salts such as $K_3PMo_{12}O_{40}$. Structure factor calculations for the potassium salt, the free acid, and the vanadyl salt revealed no significant deviations in the intensity distribution of all three structures. It is noted that the intensity distribution of all calculated diffraction patterns at low diffraction angles does not match the observations with a maximum deviation for the (110) reflection. The calculations revealed that the agreement was found to improve with a reduction of the scattering power of the cation (I(110) experimental 100%, calculated 77% for H^+, 55% for V, and 44% for K) which may be an indication that the position of the cation is not identical in phase D with the position of the potassium in the reference compound.

The assignment of phase D to a vanadyl salt of the HPA cannot be justified alone on the basis of the XRD information but relies on literature reports of NMR and EPR data suggesting the vanadium to be present in a highly symmetric chemical environment which cannot be within the Keggin anion (5, 9).

The final burst of activity followed by rapid deactivation seen in Fig. 2 is related to the occurrence of sharp reflections of phase E which is orthorhombic MoO_3. This structural disintegration of the Keggin structure above 640 K is so rapid that it cannot be resolved by consecutive diffraction scans. At 570 K the decomposition reaction can be conveniently recorded as illustrated in Fig. 7. The correspondence of the intensity changes of phase D to the simultaneously measured conversion is a good indication of the validity of the assignment of phase D as a catalytically active species. In the almost inactive state of the catalyst there is still significant intensity of phase D reflections indicating the location of the remaining active material inside or under partly converted crystals, where it is inaccessible as a surface species.

After 30 h on stream the disintegration of the crystals with the Keggin structure is almost complete and the activity has fallen to 10% of the initial value at that temperature. A close inspection of the final diffraction pattern of Fig. 7 reveals that the binary oxide MoO_3 is not isotropic but exhibits texture. All reflections with indices $h + k < 2$ and $l = 0$ exhibit asymmetric lines and an average particle size of 43 ± 3 nm whereas reflections with $l \neq 0$ are symmetric and lead to particle sizes of ca. 57 nm. These data point to irregularities in the edge-sharing connection scheme of the MoO_6 octahedra and to a nonstoichiometry of the resulting oxide. Care should thus be taken in the conclusion that this oxide is catalytically fully inactive as is known from genuine MoO_3. In the present *in situ* experiments the other components of the HPA catalyst did not give rise to crystalline phases.

The present data show that the active state of the HPA catalyst is related to a mixture of anhydride and vanadyl salt which decompose into molybdenum oxide and amor-

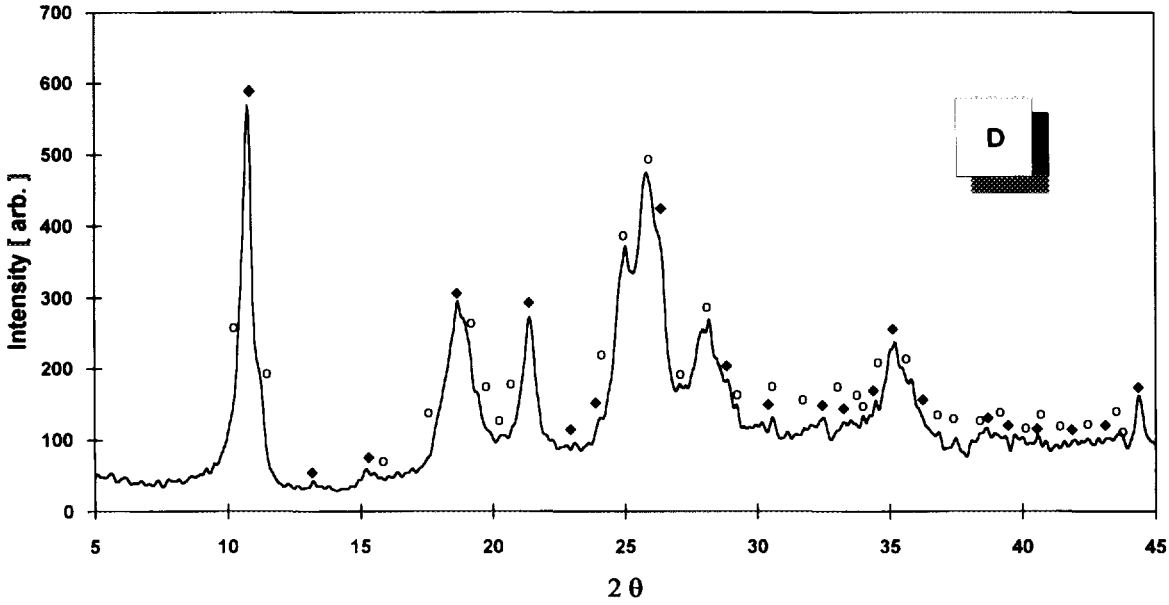

FIG. 5. Powder diffraction pattern of the vanadyl salt phase D (diamonds) at its maximum abundance in an *in situ* experiment at LHSV 1.05 and 570 K. The open circles indicate the reflections of phase C. All lines were identified from a fit of the well-resolved peaks to the respective unit cells of phases C and D (see Table 1).

phous other compounds. The conversion of the vanadium-containing anhydride into the vanadyl salt in thermal experiments was related to a threshold temperature. Under reaction conditions this temperature coincides with the onset of activity, i.e., with the dehydration of the "crystal water." The kinetics of phase transformation is, however, strongly dependent on temperature. This leads to the situation that as soon as the catalytic activity of the HPA sets in, a sequence of reactions is started leading from the anhydride over the vanadyl salt to defective MoO_3. The phase inventory of an active catalyst is thus permanently changing without a situation of steady state. We

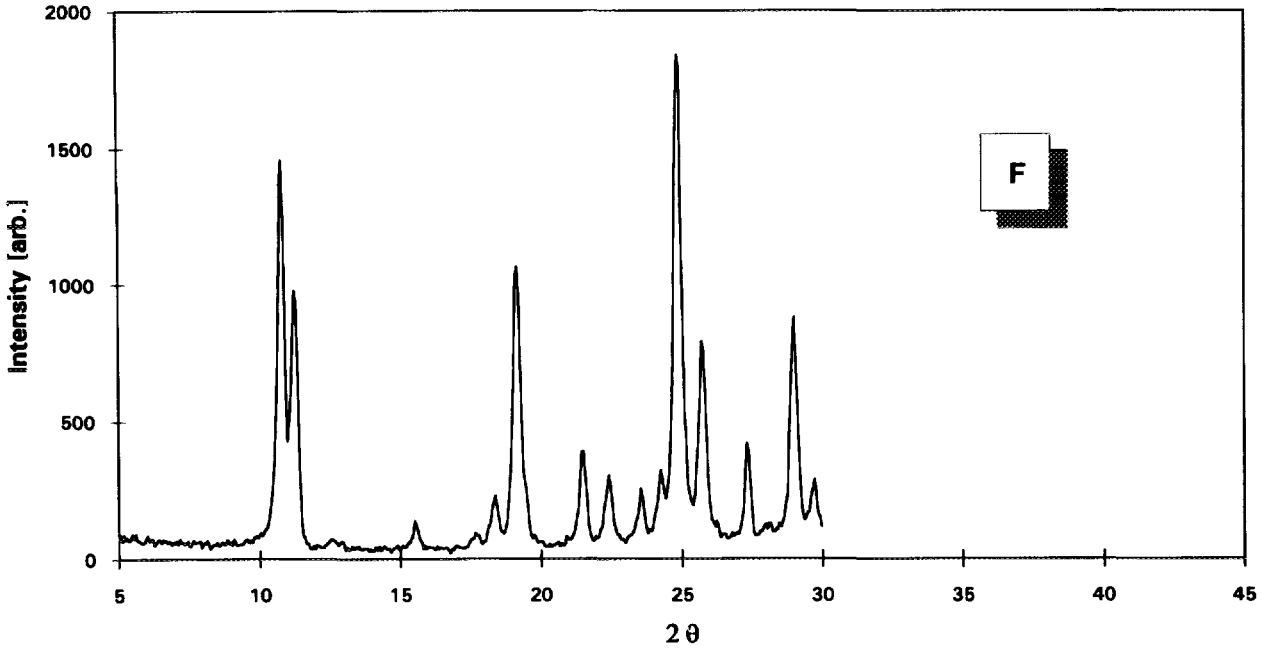

FIG. 6. *In situ* diffraction pattern of the vanadium-free unsubstituted HPA at its maximum conversion at 590 K at 2.5 LHSV catalyst load. The pattern is a well-resolved analogue to those of phase C in Figs. 4 and 5. To allow comparison of the significantly better crystallinity with the line profiles from the substituted catalysts the *x*-axis is plotted on the same scale as in Figs. 4 and 5.

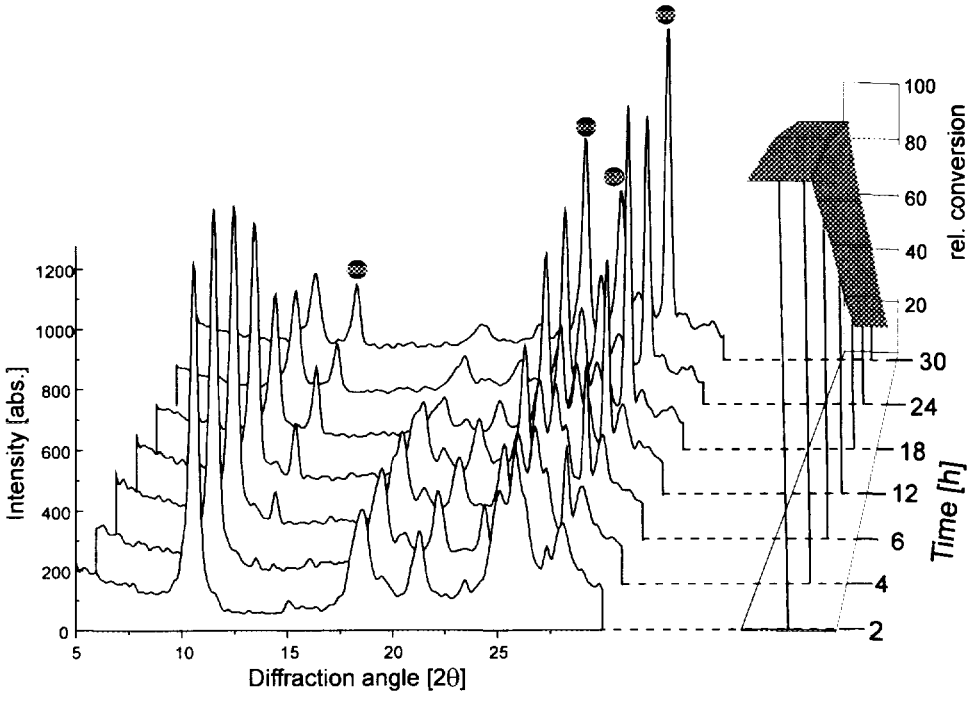

FIG. 7. Correlation of the changing catalyst structure with its conversion. Test conditions were 570 K, LHSV 2.5, and water partial pressure 50 mbar. The dotted lines arise from the decomposition product MoO_3 (phase E); all other lines arise from a mixture of phases D and C which disappear in this experiment simultaneously. The conversion drops rapidly with the occurrence of the first crystalline MoO_3.

have tested a large number of temperature programs and feed compositions which all led to this conclusion. The kinetics of the phase transformations is fast (4 h to total conversion to phase E) at high temperature (above 600 K) under high loads with IBA (LHSV 3.5 h^{-1}), after rapid dehydration and at low partial pressures of water (15 mbar). The phase decomposition is slow, on a time scale of 40 h to total deactivation at 570 K, at low catalyst load (LHSV 1.01 h^{-1}), after slow dehydration and at 50 mbar partial pressure of water. In Fig. 8 the change in phase composition is displayed under these conditions. An almost constant catalyst composition with constant conversion was observed in a time interval between 3 and 10 h. The vanadyl salt phase D decomposed then faster than the anhydride phase C. A nucleation-controlled kinetics of deactivation with an induction period may be deduced from this unsteady progress of structural transformation. The conversion to MAA followed closely the intensity drop of phase D, similar to that illustrated in Fig. 7, indicating again the close relationship between the crystalline phase composition of the material and its catalytic performance.

Water Evolution

The detection of phase transitions by *in situ* X-ray diffraction is limited by the condition that the phases must be long-range ordered. Observation of water evolution by monitoring the weight change (TGA) and by measuring the evolved gases (IMR-MS) (18) complements the structural information without the crystallinity limit.

The high-temperature section of a typical TGA experiment with a catalyst starting from the A2 phase is displayed in Fig. 9. The catalyst weight in flowing helium is not constant until 673 K where all Keggin structures are

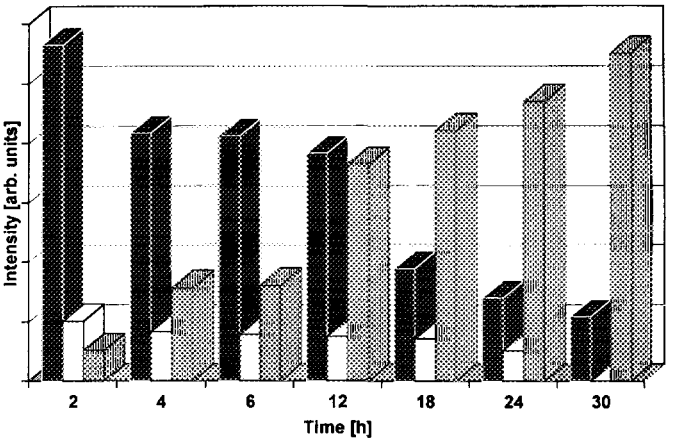

FIG. 8. Phase evolution of the vanadium-substituted HPA under mild reaction conditions (570 K, 50 mbar water, LHSV 1.05). The black bars denote the abundance of phase D, the gray bars phase E, and the light bars phase C. The intensities are integrated intensities over all reflections of the respective phase and are normalized to the specific integral intensity of each phase and a common line profile.

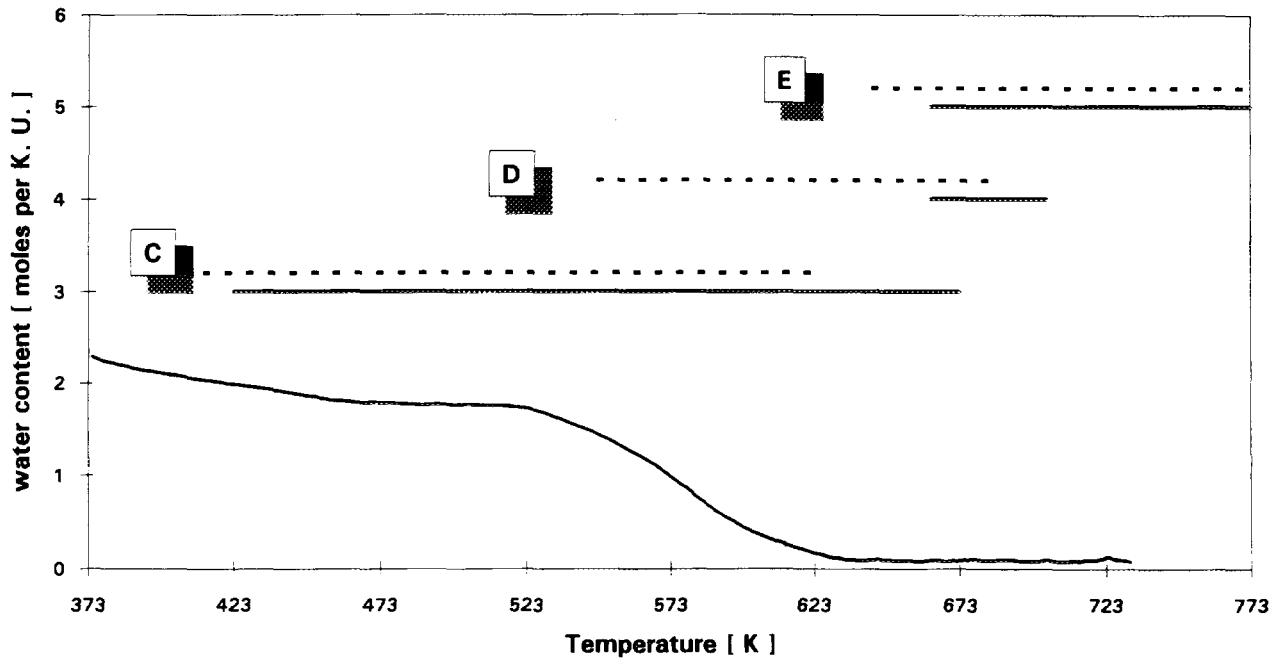

FIG. 9. Comparison of the weight loss curve of a fresh catalyst under helium with its crystal structures as function of temperature. The heating rate in the TG experiment was 5 K min^{-1}. The sample was dehydrated to phase A2 prior to the heating process by drying in flowing helium at 300 K. The dashed lines in the phase indications denote the variation in relative abundances as function of catalyst operation conditions.

destroyed to MoO_3. The continuous weight change without any plateau indicates the absence of a steady state as already found in the XRD experiments.

The most significant feature is the loss of constitutional water in a broad structure around 550 K which amounts to two formula units per Keggin anion. The broad weight loss occurs as consequence of the slow solid state reaction from the anhydride to the vanadyl salt associated with this final water loss. During the transformation which is slow, on the time scale of the heating ramp of 5 K/s, crystalline components of phases C and D coexist with their relative abundance at any given temperature depending on the time of observation. The kinetic influence accounts for the disagreement between the phase range limits by XRD and the weight loss; ideally the vanadyl phase D should result from the final dehydroxylation and not occur during the reaction. Another reason for the quantitative disagreement is the comparison of experiments under catalytic conditions (X-ray diffraction) with measurements under thermal load only (TGA). The qualitative compatibility of the comparison indicates, however, the limited effect of the reaction conditions on the phase transformation process.

Conversion of the vanadyl salt D into MoO_3 and amorphous oxides is not related to any detectable water evolution, indicating that the last protons from the Keggin ions remain in one of the decomposition products. In view of mechanistic studies of this reaction (19), the alternative explanation of a proton-free salt in the presence of molecular water and organic feed molecules is highly unlikely.

Further information can be gained from the analysis of the evolved gases from a dehydration experiment in a microreactor operated with a nitrogen gas flow with the same space velocity as in the conversion experiments. The application of the IMR-MS technique (18) allows one to simultaneously detect the evolution of water and oxygen without having to take into account possible fragmentation reactions within the mass spectrometer which could give rise to weak oxygen signals in the presence of large amounts of water. Figure 10 shows a continuous heating experiment starting from phase B of the catalyst. We detect two groups of water desorption phenomena with widely different reaction profiles. At 325 and 350 K two desorption processes with equal amounts of water (according to a curve-fitting analysis of the spectrum) occur as relatively rapid processes. The broad feature around 570 K has the same area under its peaks as one of the two low-temperature peaks, which means that at the minimum point at 460 K all material is converted into the anhydride still holding two formula units of constitutional water. Its desorption is a complex and slow process giving rise to the broad lineshape as was also observed in the TGA experiments. The shape of the low-temperature peak is compatible with a two-step dehydration process with equal weight losses.

Comparison of the water evolution with the phase ranges from XRD indicates good agreement of the dehydration process with the phase assignment. In the emis-

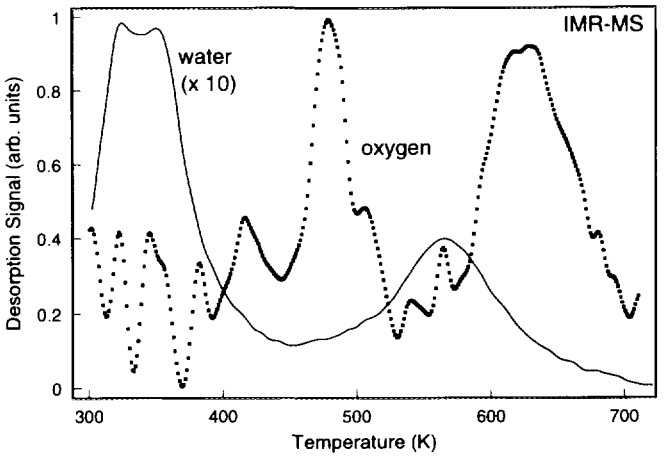

FIG. 10. Desorption of water and oxygen from a substituted HPA catalyst as function of temperature. The IMR-MS responses were simultaneously detected in a nitrogen carrier stream of 150 ml min^{-1} with a heating ramp of 3 K min^{-1}. A flow-through microreactor with a 6-mm i.d. and with 1 g of sample was used. The traces were recorded with the same instrument sensitivity with an uncorrected increased cross section for oxygen of about a factor of 4.

sion minimum around 460 K we find the anhydride phase C and above the high temperature emission maximum at 570 K the vanadyl phase D occurs. The final decomposition of the Keggin structure above 630 K is not related to significant water evolution.

Molecular oxygen is evolved around 475 K and above 580 K as shown in Fig. 10. The presence of oxygen is a clear sign of the restructuring of the Keggin units. At the onset of the vanadyl salt formation and during the final destruction of the Keggin units, irreverisible redox reactions occur under nitrogen gas. The limited oxygen partial pressure under catalysis conditions may not be sufficient to fully replenish the oxygen loss as can be concluded from the nonstoichiometry of the MoO_3 product mentioned in the lineshape analysis of its XRD pattern. The oxygen evolution is further in line with the poorly crystalline state of the MoO_3 coexisting with phases C and D, as observed in Fig. 6.

Reversibility of the Keggin Ion Decomposition

The present experiments imply that the catalysts should be largely deactivated after about 24 h on stream, if the Keggin ions accessible at the catalyst surface are the centers of catalytic activity. Literature reports (4, 20) clearly demonstrate a catalyst life much longer than the present time window. This apparent contradiction led us to perform experiments attempting to regenerate the Keggin structure. All experiments to regenerate the Keggin phases at reaction temperature *in situ* by varying the gas composition and water partial pressures within the limits of our setup were unsuccessful in presenting any X-ray diffraction evidence for an increase in abundance of Keggin structures within 24 h of regeneration time.

According to the phase analysis of Fig. 7 a deactivated catalyst should consist of a nonreacted Keggin phase in the center of each crystal protected from decomposition by a layer of nonstoichiometric MoO_3 in intimate contact with amorphous phases containing the vanadium and phosphorous from the initial Keggin material. In order to separate these components we dissolved several batches of spent catalyst in water at 330 K and monitored the UV–VIS absorption spectrum of the resulting solution *in situ* by means of a circulating system. The observed absorption spectrum shown in the inset of Fig. 11 is characteristic of the Keggin structure (21) with the absorption maximum at 310 nm occurring from the charge transfer band of octahedrally coordinated Mo^{6+}. The still-existing initial Keggin material caused part of this absorption spectrum. Unexpected, however, was the time evolution of the intensity maximum at 310 nm which increased by over two orders of magnitude within 30 min as displayed in the main plot of Fig. 11. The intensity evolution can be divided into three regions. The rapid initial increase is due to the solution of existing Keggin material in the interior of each catalyst particle. The second phase between 5 and 20 min can be ascribed to the conversion of partly defective lacunar Keggin units back to the most stable $PV_1Mo_{11}O_{40}$ species. This reaction, which is also part of the synthesis process, was also observed to occur in ^{31}P NMR experiments which will be described in detail elsewhere (22). The third period of slow increase in the 310 nm absorption extends over 1400 min and is associated with the regeneration of Keggin units from the defective, partly reduced, and amorphous oxide materials. This is a reaction similar to the hydrothermal synthesis reaction, occurring at somewhat lower temperature due to the higher reactivity of the intimately mixed and defective oxides compared to the well-crystallized, fully oxidized, and coarse starting mixture. The experiment clearly establishes the existence of a regeneration process starting from a mix of precursor structures which leads to the restructuring of the Keggin anion.

Crystallization of the used catalyst solution at 300 K produces a greenish-colored material exhibiting in water vapor the fully hydrated normal Keggin phase in its cubic structure. The regeneration process has thus changed the starting compound from the tetragonal A1 phase into the cubic phase, normally characteristic of unsubstituted Keggin ions. EDX analysis of the crystals showed that each crystal did contain vanadium in the expected abundance. Such a change in the polymorph of the material was already noted in our previous single crystal study (5) where it occurred after the addition of copper as counterion. In the present case we attribute the polymorphism

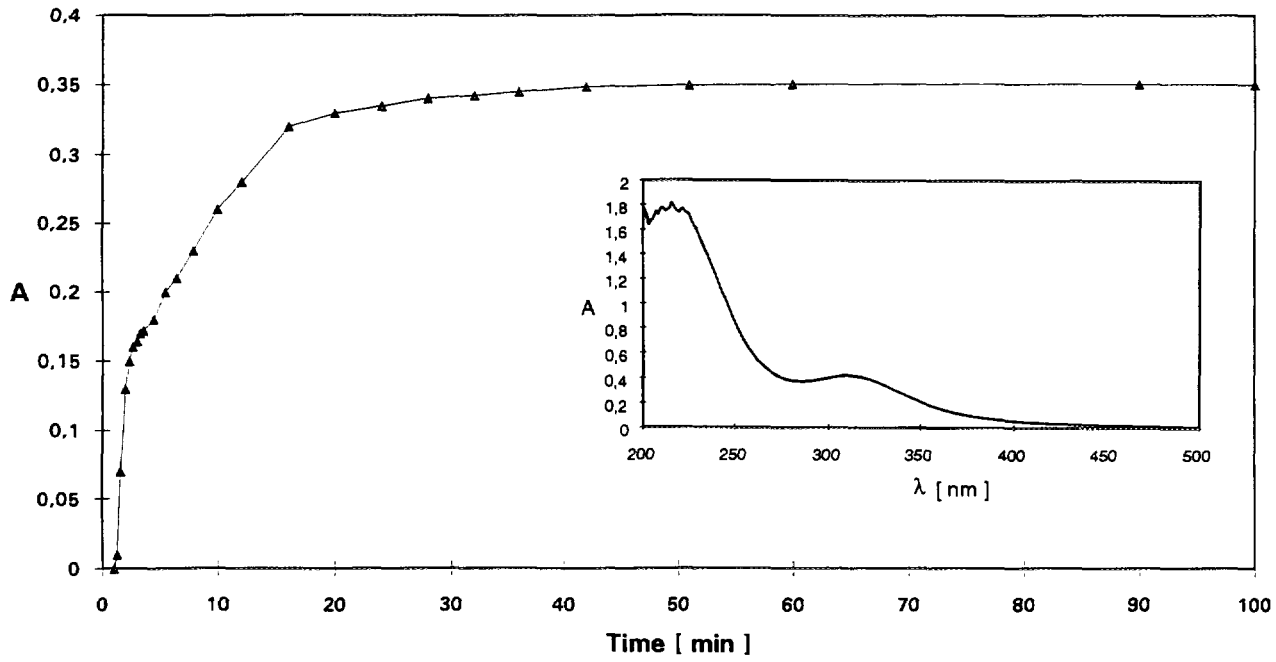

FIG. 11. Evolution of the UV–VIS absorption at 310 nm as function of time. A sample of deactivated substituted HPA is dissolved in water at 323 K. The inset shows the whole absorption spectrum characteristic of the Keggin anion. The data were obtained in a circulation setup with constant temperature in all sections of the dissolution vessel and the analytical apparatus. The final concentration of Keggin anions is about 0.01 mol/liter.

to a partly reduced Keggin anion as the solution and the crystals showed the green color characteristic of the presence of some reduced Mo centers. We exclude the possibility of a vanadium salified normal HPA from the absence of excess vanadium ions in the mother liquor.

Ex situ tempering at 473 K in air and rehydration at 300 K transformed the regenerated material in a well-crystallized mixture of both polymorphs, the tetragonal phase A1 and the cubic normal Keggin structure, as can be seen from the diffraction pattern in Fig. 12. There are no unindexed reflections and no traces of MoO_3 or amorphous components left in this diffraction pattern, documenting the efficiency of the restructuring process. From this we conclude that oxidation at elevated temperatures in air was necessary to produce the inverse Keggin structure (5) during regeneration. The yellow color of the material gave no evidence for the presence of reduced molybdenum species after the tempering process. Immediately after the catalytic testing the catalyst was dark green-bluish in color and remained so after dissolution in water at 330 K in air.

Micromorphology and Homogeneity

In the literature (12) it was reported and later quoted (23) that spent HPA catalysts undergo a morphological transformation into a featureless smooth state which was termed amorphous and from this it was concluded that the crystal structure should also become amorphous. The term "pseudoamorphous" (23) was used to describe the state of the catalyst in which the Keggin anions should be still present but the long-range order created by the hydration water is lost. This state of the catalyst is in fact identical to phases C and D found in the present study but these states are not amorphous, as can be seen from, e.g., Figs. 5, 6, and 7. The series of survey SEM images presented in Fig. 13 was taken to clarify the correlation between catalytic activity and morphology. The top image shows the catalyst in its fresh state exhibiting the structure A2. It presents itself as a compact assembly of well-crystallized plates exposing sharp edges with very low intergrain porosity. After activation in its still active state the morphology is quite different as can be seen from the central plate in Fig. 13. Large spherical aggregates of a variety of small crystal habiti of platelets and more needle-like forms are now present exposing significant intergrain porosity. High-magnification images reveal an overall good crystal quality with smaller crystals covering many faces of the larger individuals seen in Fig. 13. In its fully deactivated state (Fig. 13, bottom) the catalyst has changed its morphology again and occurs as a mixture of platelets and needles as seen in the active state embedded in a matrix of apparently solidified featureless material which is reminiscent of the image shown by Centi *et al.* (12). X-ray diffraction of this stage shows little indication, however, of large amounts of amorphous matter, as can

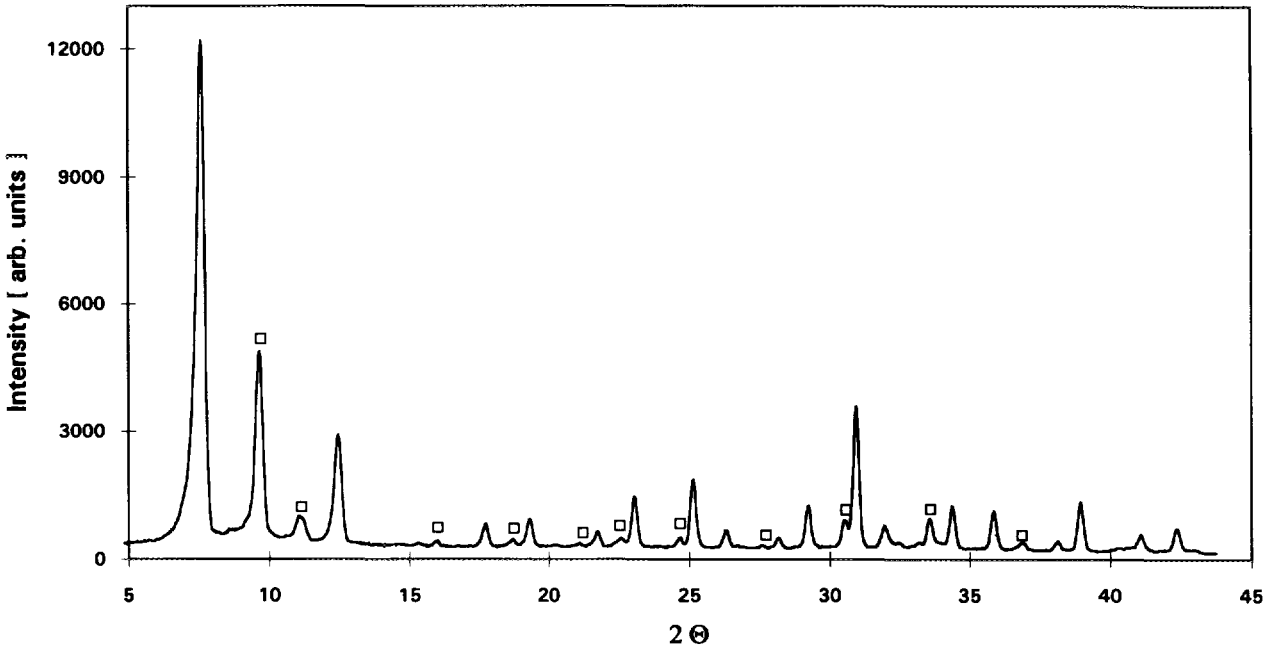

FIG. 12. Powder diffraction pattern of the fully hydrated state of the restructured substituted HPA after a thermal treatment at 473 K in air. The squares denote the reflections of the initial tetragonal inverse Keggin phase (A1); the unlabeled reflections all arise from the cubic Keggin structure.

be seen from, e.g., Fig. 7. We recall that the fully decomposed catalyst contains no phases of phosphorous and vanadium which must thus be present as X-ray amorphous material, possibly identical with the featureless material seen at the bottom of Fig. 13.

In order to analytically characterize the materials, microbeam EDX experiments were performed as point analyses on very small and thin particles which were selected to ensure a bulk representation of the chemical composition. The fresh catalyst was fully homogeneous and of exactly the Mo : P : V composition as expected. The used and spent catalysts were not homogeneous as can be seen from typical analysis data presented in Figs. 14 and 15. Figure 14 was obtained from one thin platelet which was part of a larger agglomerate. The smooth and isolated part of this particle was used for the point analyses. All results were independent of the particle orientation in the microscope after the appropriate ZAF corrections. The data show that the molybdenum content is homogeneous and close to the stoichiometric value. Phosphorous is always present in significant excess and vanadium occurs in variable amounts. No morphological contrast was detectable that would indicate the presence of multiple crystals. The consequence would be that the platelet itself is inhomogeneous. This implies that each crystal, which is much larger than the crystallographic size of single crystals (X-ray line broadening), is composed of a number of domains with different chemical compositions. The phases detected in the XRD experiment are then present within each catalyst crystal without a macroscopic spatial phase separation. The EDX "point" analyses average over several such domains because the area of X-ray excitation in this material is certainly larger than a few nanometers which was found to be the size of the domains from the X-ray diffraction linewidths. The large variation in chemical composition is thus explained.

In the deactivated state the microheterogeneity is even more pronounced. The chemical composition over a platelet of similar morphology varies significantly more than in the still active state. In Fig. 15 this variation is shown, as well as the now detectable microheterogeneity of the platelet. Some internal structure can be identified in addition to smaller platelets at its periphery which may have grown from domains of different chemical composition. Neither in any small particle nor in point analyses directly aiming at amorphous regions were we able to find direct proof for the absence of Mo in the amorphous phase as was suggested from the X-ray diffraction argument. In the deactivated state the elemental composition is drastically more heterogeneous than in the active or even the precursor state. No evidence was found, however, to ascribe the amorphous morphology to a single phase; the embedding material may be enriched in P + V components but is not free of Mo which may be present as small MoO_3 particles not giving rise to a morphological structuring detectable in the SEM.

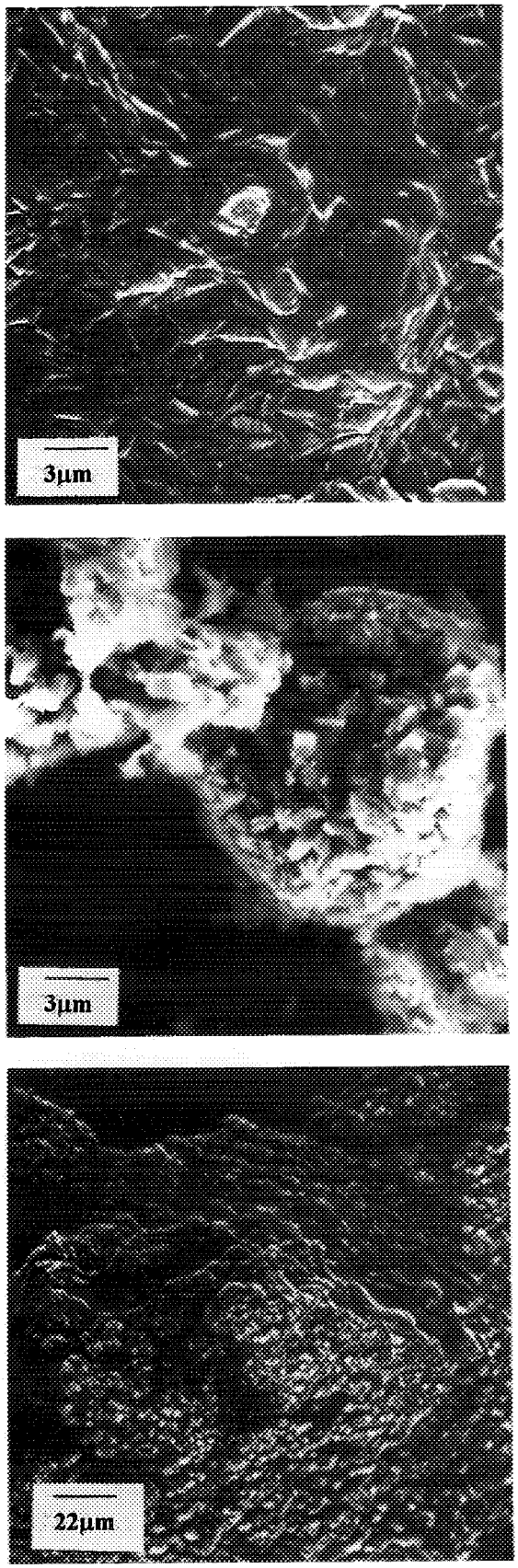

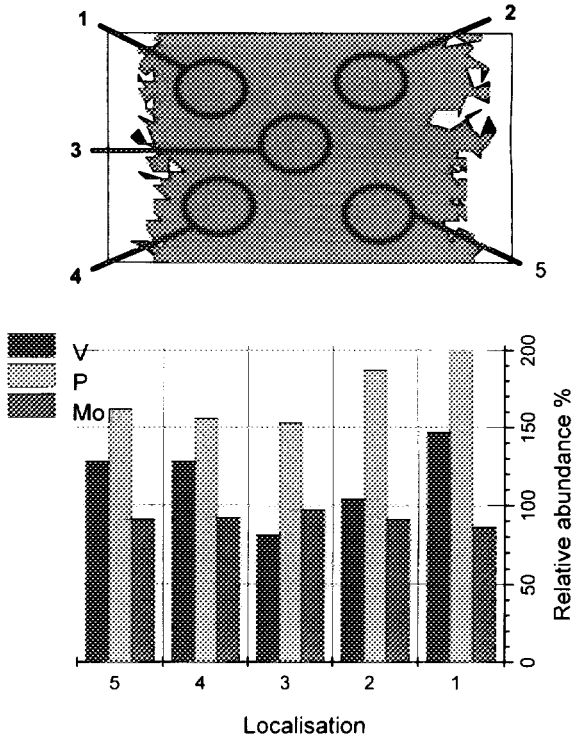

FIG. 14. Microanalytical data of a small particle of the activated HPA. The schematic representation of the contours contain the locations of point analyses. A microfocused beam of 25 kV electrons and 70 nA current was used for excitation. The numbers in the bar diagram are relative atomic concentrations normalized to the nominal stoichiometry of the HPA (100% for each element). The K emission lines for P and V and the L emission line for Mo were used for the quantitative analysis. An image magnification of 4000 was used for the analysis.

In summary, the SEM data indicate a morphological and chemical heterogeneity of the dehydrated HPA present in the active and deactivated state. Each individual crystal seems to consist of domains of chemically different phases in the active state. In the deactivated state these domains are separated into larger crystallites of different composition and into an amorphous component consisting of all three heavy elements in a composition which cannot crystallize.

Postmortem Analysis of Practical Catalysts

In order to validate our results for materials used under technical conditions we analyzed two samples on Kieselgur supported catalyst systems used for 200 and 3800 h under conditions similar to those described in the literature (4). The short run was dedicated to our analysis and the sample was thus isolated with great care, allowing no

FIG. 13. SEM survey images of fresh HPA (top), after activation at 570 K for 4 h (center), and after full deactivation at 570 K (bottom).

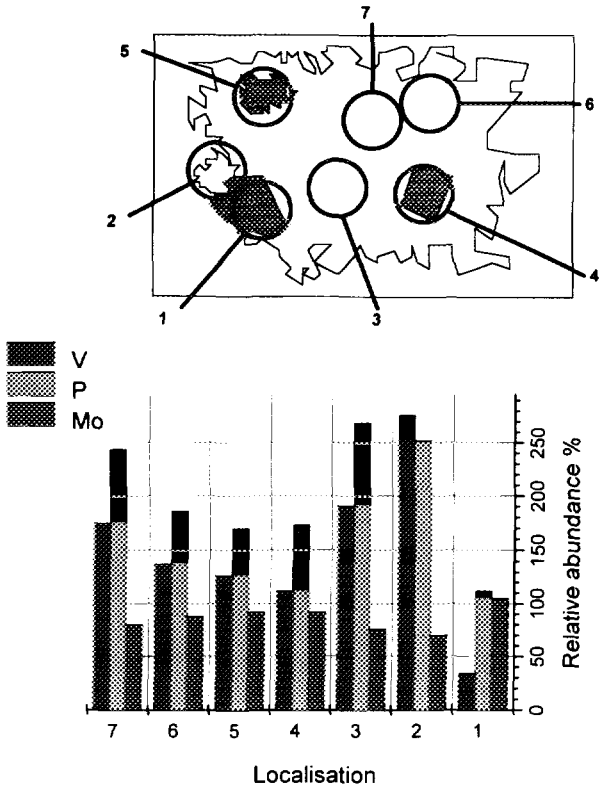

FIG. 15. Microanalysis of a platelet of the fully deactivated catalyst. For details of the analysis see Fig. 14.

intermixing with nonrepresentative head/tail materials, and was kept under nitrogen all time. The long-term sample was taken from a pilot plant test and was stored for several weeks prior to structural analysis. Both catalysts were, at the time of sample collection, still active and produced MAA at higher selectivity than in our *in situ* tests. In Fig. 16 the analyzed diffraction patterns are shown. We identified well-crystallized catalyst materials and observed strong reflections from the support (labeled K). The phase inventory is the same as found in our *in situ* experiments with the short-run sample exhibiting a dominant abundance of phase D (diamonds). The long-used sample contains predominantly the decomposition product E (labeled M). Phase C is not detectable in large abundance but we see reflections (unlabeled) of phase B indicating that during sample collection a partial rehydration of phase C to phase B had occurred.

These data are strong support for the *in situ* character of the present experiments and the relevance of our findings. Taking into account the transport limitation in our *in situ* experiments in the regime of formation of phase D and its predominant occurrence in the postmortem samples, it seems likely to assign the active phase of the catalyst to phase D.

DISCUSSION

The correlation of *in situ* powder diffraction with simultaneous observation of the catalytic activity of the HPA system has revealed the following points relevant for the understanding of the mode of operation of this catalyst. The phase analysis was complemented with integral thermal analysis methods under only thermal loads. The good agreement of all data indicates that the scenario of phase conversions can occur only from thermal load and is thus inevitable. The presence of the organic materials of catalytic conversion reduces, however, the temperatures of the solid state reactions and influences the ranges of stabil-

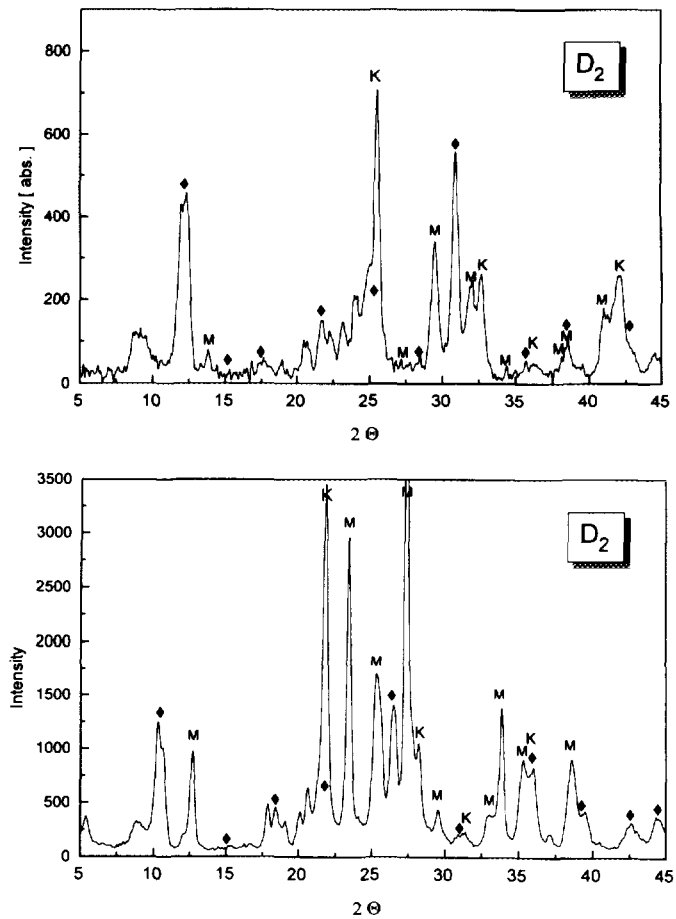

FIG. 16. Transmission XRD traces of used supported catalysts. The top trace was obtained from a sample run for 200 h in a laboratory test reactor under conditions described by Emig *et al.* The HPA was supported on Kieselgur (reflections labeled K). The material was collected under nitrogen after shutting off the hot reactor under nitrogen. The bottom trace was obtained from a pilot plant test operated over 2000 h. The sample was obtained under no defined shut-off conditions and kept in laboratory air for weeks before analysis. The diamonds designate reflections of phase D, reflections of phase E are labeled "M." The top trace was collected using Co*K* alpha radiation, for the bottom trace conventional Cu*K* alpha radiation was employed.

ity of individual phases, which is an indication for the involvement of parts of the crystal structures in the catalytic process. The present experiment cannot distinguish between destabilizing effects of cation reduction or oxygen anion removal.

Hydrated phases with crystallization water are inactive in the IBA oxidehydrogenation. In the temperature window of practical operation the catalyst is not a single-phase material. A mixture of the anhydride phase (C) and the novel cubic vanadyl salt phase (D) can be observed in different relative abundances depending on the thermal prehistory and the conditions of conversion of the catalyst.

One active phase is the vanadyl salt of the HPA anhydride. This conclusion is in line with a recent report (23) by Casarini *et al.*, who showed the existence and catalytic activity of such phases indirectly by spectroscopic techniques.

The catalyst system is not structurally stable under any conditions of finite conversion; i.e., it changes its phase inventory continuously. This is an indication that no single bulk phase is the active species but rather both HPA phases (C and D) are active with probably different reaction pathways and hence different activities and selectivities (23) as was also concluded by Kutyrev *et al.* (24) from the localization of the substituting element V inside (phase C) or outside (phase D) of the Keggin anion. Most relevant is the finding that the phase mix of the active catalyst is under optimized reaction conditions (including all components of the technical feed) unstable and decomposes into crystalline but defective molybdenum oxide as the only phase detectable by X rays. There seems to be no way to profoundly influence or even suppress the long-term deactivation by further modification of the operation conditions given that high catalyst loads are desired.

Microanalytical data show that the solid state reactions also give rise to severe morphological modifications and an increasing demixing of the atomically dispersed constituents from the initial homogeneous Keggin crystals.

The changing phase inventory of the active catalyst allows one to understand the shape of the conversion versus temperature curve of Fig. 2. It is composed of a step function related to the presence of the anhydride (C) superimposed with a rising contribution from the intrinsically more active vanadyl salt (D). As its abundance is more rapidly reduced than that of the anhydride (Figs. 6 and 8) a second plateau in the temperature region of industrially optimized operation is observed. The sharp final rise of activity related to the formation of crystalline MoO_3 (E) may be understood by the inevitable increase in active surface area caused by the decomposition of the Keggin structure.

This pattern of reactivity may occur with its parameters described as a consequence of the special conversion conditions in our experiment. Under integral reactor conditions a different time scale and complete interconversion of phases C and D may occur. The present reaction profile may be regarded as a good model for the events taking place in the migrating hot spot region of the reactor.

During crystallization of the at-first nanocrystalline and nonstoichiometric molybdenum oxide (see Fig. 5) the crystals of Keggin anions will disrupt and exhibit an increased interface area. This becomes evident from a morphological analysis of catalysts used for prolonged times in integral reactor experiments. The HPA crystals are fully disrupted and have reagglomerated with a much smaller particle size as seen in Fig. 13, leaving uncovered large patches of the initially homogeneously covered support. As the total BET area of the catalyst sample is low ($1.5\ m^2/g$) this effect is significant and may account for the factor of 2 increase in activity. The initial nanocrystalline nature of the final product molybdenum oxide further allows one to understand its reactivity toward formation of volatile complexes of reduced Mo-organic species (4, 19).

The Keggin anion structure becomes metastable in its dehydrated form under reducing conditions as well as under thermal load only. The water in the feed has not the function of maintaining a stable hydrated form of the HPA (25), where under complete hydration it effectively blocks the adsorption of the organic substrate (26) but is likely to influence the catalytic cycle itself, e.g., by lowering the desorption energy of the product (27) by competitive adsorption on an active center on the Keggin anion (28). That the Keggin anion contains the active center seems almost certain according to the experiments presented where high MAA yields were correlated with crystalline phases. Water addition to the feed, acting as diluent and regulating the catalyst load, was further found to be an important function of this additive.

Observation of molecular oxygen evolution in the temperature range of catalytic action at purely thermal load is an indirect confirmation of the possible mode of action of Keggin anions in supplying activated oxygen to the organic substrate (29). The oxygen evolution under thermal load is one reason for the limited effect of the presence of reducing chemicals on the phase transformations. The presence of molecular oxygen in the gas phase may counteract the decomposition of Keggin anions in reducing or oxygen-free atmospheres if the losses are reversible at reaction temperatures. These observations are in line with literature reports about the reactivity of oxygen constituting the Keggin ions based on infrared spectral data (30) and a model reduction with hydrogen.

In a fundamental study of the application of unsubstituted HPA in the oxidation of IBA by McGarvey *et al.*

(31) the direct involvement of lattice oxygen in the partial oxidation was shown. In depletion experiments with the free acid catalyst and several salt forms only the organic feed was used without dosing oxygen. The initially active catalysts declined in performance to total deactivation after 4 h on stream. In postmortem analyses the authors noted no structural changes by XRD after this deactivation. This statement is not in contradiction to the present findings if the *ex situ* conditions are taken into considerations. After the mild catalyst loads the samples were allowed to cool and were then exposed to air and analyzed in air giving the structurally destroyed parts of the material ample opportunity to regenerate into a state where no structural defects were observable.

The molecular nature of phase D is only approximately given by the term "vanadyl salt." Powder X-ray diffraction alone is an insensitive tool for discriminating a single Keggin phase from a "mixed crystal" situation in which the anhydride and a completely salified phase coexist. Although our micro-EDX data exclude large-scale phase separation, such a two-phase situation may exist within grains of the catalysts or even on the level of individual domains. The crystal quality of the *in situ* products is poor enough to accommodate several possible models of mixed crystals. It is pointed out that a similar two-phase material was found in a recent detailed analysis (32) of earth alkaline derivatives of the Al compound.

The kinetics of deactivation clashes with reported times on stream for pilot plant tests of over 2000 h under heavy catalyst load. The only possibility to account for this is to assume that a solid state reaction occurs within the catalyst bed allowing one to regenerate the Keggin structure from the defective MoO_3 and the amorphous other components. Model experiments with deactivated catalysts showed the strong possibility for a regeneration of the catalyst during the operation, although maybe not in a well-crystallized form detectable by X-ray diffraction. It is important to note that water is the essential ingredient to allow the self-reorganization of defective oxidic materials and partly disrupted Keggin cages into the highly complex but obviously thermodynamically most stable perfect Keggin structure.

The failure to observe the restructuring process directly *in situ* by X-ray diffraction is traced back to an insufficient water vapor pressure in our reaction chamber which is limited by its design to below 100 mbar. Work is in progress to remove this limitation.

On the basis of the present experiments nothing can be said about the time scale of the structural transformations under practical reaction conditions. The limitations of our experiments do not allow us to conclude that the critical time of ca. 30 h will necessarily be realistic although the agreement with the time scale of the hot spot migration (16) may not be circumstantial. In any case we could show that the result of the structural transformation is the same in integral reactor testing (*ex situ*) and in the present *in situ* experiments.

The role of the vanadium in the catalytically active state of the material cannot be only the modification of the electronic structure of the Keggin anion as is in one active phase the vanadium is not incorporated in the ion. As a counterion it modifies the electrostatic interaction between the Keggin ion and its environment as discussed by Casarini *et al.* (23). The modified stability of the hydration states with changing V contents (5) is a different effect related to the presence of the V inside the Keggin unit modifying the charge-to-radius ratio of the whole unit. In both localizations V modifies the acid properties of the Keggin units. The presence of vanadium is beneficial but not, however, essential to the operation of the catalyst, allowing one to speculate that it may act in its counterionic state as a sink for electrons thus extending the life of the Keggin ion under reducing conditions of catalytic action. A possible further role of vanadium relates to the operation of the restructuring process for the Keggin structure for which vanadium was found to be a catalyst (22). In this sense the vanadium would act as a structural rather than an electronic promoter.

In conclusion, the present work focusing on the bulk structural aspects of HPA application has shown that the complicated hydrated microporous forms of the present HPA are catalytically inactive in the selective oxidation of IBA. The removal of the hydration water creates catalytic activity involving the bare Keggin ions with or without the constitutional water. Simultaneously, a sequence of solid state reactions is put into operation. It involves the expulsion of the substitutional vanadium in the counterion position of the Keggin structure, the activation of some structural oxygen, and the detrimental conversion into MoO_3 and amorphous other phases. The whole process is thermally initiated and only moderately influenced by the gas phase composition in the window of catalytic application. Even without any catalytic load, the Keggin structure would decompose. Attempts to solve the problem of insufficient long-term stability by preserving the initial Keggin structure as long as possible by structural promoters are likely to fail. The instability is an intrinsic property of the system.

The preparation of phase-pure single crystals of any of the active phases and their precise structural characterization by X-ray diffraction will be very difficult as rapid phase preparation (to prevent conversion reactions) is incompatible with the growth of good quality crystals.

Self-reorganization of the decomposition products into the initial HPA seems possible in the presence of sufficient water partial pressure. It is essential, however, that no

significant spatial separation of the ingredient phases (which may be overcome by dissolution in liquid water) has occurred. Such a spatial disintegration would be the consequence of the growth of large and well-ordered crystals of MoO_3 which represents the one way of final and irreversible deactivation. Transport reactions of any component via the gas phase under the participation of organic ligands as "volatilizers" are further processes contributing to the long-term deactivation. One strategy to improve the catalyst lifetime is thus to influence the solid state reaction kinetics leading to well-ordered deactivation products. Growth inhibitors for MoO_3 would act as potent structural promoters.

ACKNOWLEDGMENTS

This work was done in collaboration with Röhm AG (Darmstadt). We acknowledge fruitful discussions with E. Bielmeier, Th. Haeberle, and H. Siegert. A fruitful exchange of information and of catalyst samples with G. Emig (Erlangen) and his group is also acknowledged. Financial support came from the Röhm Foundation, from Du Pont (Germany), and from the Fonds der Chemischen Industrie.

REFERENCES

1. Misono, M., *Catal. Rev. Sci. Eng.* **29,** 269 (1987).
2. Pope, M. T., and Müller, A., *Angew. Chem.* **103,** 56 (1991).
3. Akimoto, M., Shima, K., Ikeda, H., and Echigoya, E., *J. Catal.* **86,** 173 (1984).
4. Watzenberger, O., Emig, G., and Lynch, D. T., *J. Catal.* **124,** 247 (1990).
5. Herzog, B., Bensch, W., Ilkenhans, Th., and Schlögl, R., *Catal. Lett.* **20,** 203 (1993).
6. Mioc, U., Davidovic, M., Tjapkin, N., Colomban, Ph., and Novak, A., *Solid State Ionics* **46,** 103 (1991).
7. Izumi Y., Urabe, K., and Onaka, M., "Zeolite, Clay and Heteropoly Acid in Organic Reactions." VCH Verlag, Weinheim, 1993.
8. Misono M., *in* "Proceedings of Climax, 4th International Conference on the Uses of Molybdenum, Ann Arbor, Mich., 1982" p. 289.
9. Fournier, M., Feumi-Janou, Ch., Rabia, Ch., Herve, G., and Launay, S., *J. Mater. Chem.* **2,** 971 (1992).
10. Taouk, B., Ghoussoub, D., Bennai, A., Crusson, E., Rigole, M., Aboukais, A., Decressain, R., Fournier, M., and Guelton, M., *J. Chim. Phys.* **89,** 435 (1992).
11. Rocchiccioli-Deltcheff, C., Fournier, M., Franck, R., and Thouvenot, *Inorg. Chem.* **22,** 207 (1983).
12. Centi, G., Lopez Nieto, J., Iapalucci, C., Brückman, K., and Serwicka, E. M., *Appl. Catal.* **46,** 197 (1989).
13. Brückman, K., Tatibouet, J. M., Che, M., Serwicka, E., and Haber, J., *J. Catal.* **139,** 455 (1993).
14. Black, J. B., Clayden, N. Y., Gai, P. L., Scott, J. D., Serwicka, E. M., and Goodenough, J. B., *J. Catal.* **106,** 1 (1987).
15. Herzog, B., Ilkenhans, Th., and Schlögl, R., *Fresen. J. Anal. Chem.* (1994), in press.
16. Haeberle, Th., and Emig, G., *Chem. Eng. Technol.* **11,** 392 (1988).
17. Rocchinoli-Deltcheff, C., Thouvenot, R. R., and Frank, R., *Spectrochim. Acta A* **32,** 587 (1976).
18. Tegtmeyer, U., Weiss, H. P., and Schlögl, R., *Fresen. J. Anal. Chem.* **347,** 263 (1993).
19. Ai, M., *J. Catal.* **98,** 401 (1986).
20. Watzenberger, O., Dissertation, Erlangen, 1991.
21. So, H., and Pope, M., *Inorg. Chem.* **11,** 1441 (1972).
22. Ilkenhans, Th., and Schlögl, R., submitted for publication.
23. Casarini, D., Centi, G., Jiru, P., Lena, V., and Tvaruzkova, Z., *J. Catal.* **143,** 325 (1993).
24. Kutyrev, M. Yu., Staroversova, I. N., Thiep, N. Z., and Krylov, O. V., *in* "New Developments in Selective Oxidation" (G. Centi and F. Trifiro, Eds.), p. 869. Elsevier, Amsterdam, 1990.
25. Furuta, M., Sakata, K., Misono, M. and Yoneda, Y., *Chem. Lett.* 31, (1979).
26. Ernst, V., Barbaux, Y., and Courtine, P., *Catal. Today* **1,** 167 (1987).
27. Watzenberger, O., and Emig G., *in* "New Developments in Selective Oxidation by Heterogeneous Catalysis" (P. Ruiz and B. Delmon, Eds.), Studies in Surface Science and Catalysis, Vol. 72, p. 71, 1992.
28. Serwicka, E. M., *Z. Phys. Chem* **152,** 105 (1987).
29. Taketa, H., Katsuki, S., Eguchi, K., Seiyma, T., and Yamazoe, N., *J. Phys. Chem.* **90,** 2959 (1986).
30. Eguchi K., Toyozawa Y., Yamazoe N., and Seiyma T., *J. Catal.* **83,** 32 (1983).
31. McGarvey, G. B., and Moffat J. B., *J. Catal.* **132,** 100 (1991).
32. McGarvey, G. B., Taylor N. Y., and Moffat, J. B., *J. Mol. Catal.* **80,** 59 (1993).